Flow Structures over Fixed 2D Bedforms in Transient States

C.A. Unsworth[1], D.R. Parsons[1], A.J.H. Reesink[1], J.L. Best[2], P.J. Ashworth[3] and R.J. Hardy[4]

1. Department of Geography, Environment and Earth Sciences, University of Hull, Hull, HU67RX, UK [*]E-mail: C.A.Unsworth@2011.hull.ac.uk
2. Departments of Geology, Geography and Geographic Information Science, Mechanical Science and Engineering and Ven Te Chow Hydrosystems Laboratory, University of Illinois at Urbana-Champaign, 1301 W. Green St., Urbana, IL, 61801, USA
3. Division of Geography and Geology, School of Environment and Technology, University of Brighton, Brighton, Sussex, BN24GJ, UK
4. Department of Geography, University of Durham, Durham, DH13LE, UK

Abstract

Flow processes measured in the laboratory over fixed, 2D or 3D bedforms have mostly been conducted at one flow depth and with bedform dimensions set by scaling laws based upon "equilibrium" flow conditions. These results thus have limited applicability to many natural situations where bedforms and flow fields are co-evolving at different rates in response to transient conditions, such as changes in flow depth and flow discharge associated with a flood. The research presented herein investigates flow processes over 2D fixed bedforms under a range of non-equilibrium, transient, states in order to quantify the spatio-temporal changes in turbulence associated with steady conditions that are set at non-equilibrium depths and velocities. Flow field information was obtained at steady states for a range of flow depths and mean flow velocities, mimicking conditions during the transient evolution of flow and bedforms during a flood wave. This allowed quantification of flow fields over bedforms under transient boundary conditions, including shear stress profiles and the spatial variation in the dynamics of the separation zone. These findings provide data for a preliminary assessment of the link between sediment transport lag and transient flow dynamics, and facilitate an analysis of the implications of variable dune height: flow depth for flood wave propagation and bedform response.

1. INTRODUCTION

The flow structure over dunes has been extensively measured in laboratory conditions and there is general agreement on the nature of the flow field over idealised dune forms (e.g. Nelson et al., 1993; Nezu and Nakagawa, 1993; McLean et al., 1994; Bennett and Best, 1995; Nelson et al., 1995; Kadota and Nezu, 1999; Fedele and Garcia, 2001; Best, 2005a,b; Garcia, 2008). However, these laboratory experiments have only quantified the flow fields over dunes in steady flows that are scaled to a flow-morphology equilibrium condition. Detailed understanding of flow-bedform interactions during unsteady or transient conditions, which commonly results in a flow-morphology hysteresis, is currently lacking. Yet the quantification of such flow-form interactions is vital to understand these unsteady dynamics and mutual adjustments that occur in natural flows.

It is well known that stoss side flow acceleration and lee side flow separation associated with dunes produces shear layer turbulence and fluid ejections (e.g. Bennett and Best, 1995) and that the point of flow reattachment may be important in suspending large quantities of bed sediment. However, there is currently a lack of understanding on how these processes change when the flow and bedforms are not under scaled equilibrium conditions. This research aims to investigate how the flow structure over fixed, idealised, 2D dunes changes with variations in flow depth and flow velocity.

2. METHODS

A large recirculating flume that had dimensions 1 m wide, 1 m deep, and 10 m long was used herein. Three 2D idealised dune forms were fixed to the flume bed. They were 0.08 m high and with an angle-of-repose lee face (~30 degrees), and a crest to crest wavelength of 0.80 m. Detailed two-dimensional (streamwise (u) and vertical (w)) flow velocities were quantified using a Dantec 100 Hz Particle Imaging Velocimetry (PIV) system. The PIV was positioned along the centreline of the flume and centred on the mid-stoss of the third dune form. Velocities were measured for ~130 seconds per run, yielding an array of ~9000 images at 1280x800 pixels. Vectors were calculated using an adaptive correlation on a 32x32 grid, with sub-pixel

refinement. Outliers were identified and replaced by a combined automated penalised least squares approach with a discrete cosine transform and cross-validation (Garcia, 2011).

A suite of experimental conditions were investigated using this set-up, where the depth and/or flow velocity were systematically changed over the same fixed bedforms. Herein, we present results on the first 5 experiments conducted, at 0.28m flow depth (Table 1).

Table : List of experimental conditions. No.= run number, D = average flow depth (m), Ū = depth-averaged flow velocity over crest (ms^{-1}) , Fr = Froude number, Re = Reynolds Number, Q = discharge (m^3 s^{-1})

No.	D	Ū	Fr	Re	Q
1	0.28	0.14	0.08	38535	0.039
2	0.28	0.30	0.18	83218	0.083
3	0.28	0.70	0.42	194491	0.195
4	0.28	0.76	0.46	213297	0.214
5	0.28	0.92	0.56	258427	0.259

3. RESULTS

3.1. Mean velocities

Figure 1 (see end of article) shows the time-averaged normalised flow velocity profiles for the streamwise and vertical components of flow for several locations across the dune. For the streamwise velocity, *u*, the largest variation in the shape of the velocity profile between all the runs occurs over the crestal locations (Fig. 1 A), although there is no obvious trend with increasing flow velocity.

The mean velocity over the trough and near the reattachment point along the dune (Fig. 1 C, E) shows similar shaped profiles of streamwise velocity, notably at and beneath the shear layer (Fig. 1 C), but with a slight variation above the distinct kink in the profiles. The spatial variation in mean *u* on the stoss slope shows the impact of the lee side wake layer on the recovery of the time-averaged flow field, with the highest *u* velocities systematically shifted into the upper portions of the profile along the stoss side.

The vertical (*w*) component of velocity shows significant spatial variation along the dune and between each of run conditions (Figure 1, B,D,F,H,J). Although the shape of the normalised vertical velocity profiles converges towards the bed between the various conditions, there are significant divergences above this zone, which show a systematic trend with changing flow conditions. The normalised vertical velocity profiles in the dune trough (Figure 1D) are largely consistent until the shear layer (around crest height, at x=200), showing how strongly coupled the flow field is to the bedform morphology. However, the shape of the vertical flow profile for the different incoming velocities changes dramatically around the reattachment point. This is a key indication of where, and how much, flow is directed towards the bed on the stoss side of the dune within the region of flow recovery.

This result indicates that there is a substantial variation in normalised flow directed towards the bed with increasing flow velocity, and thus the spatial location of the maximum bed shear stress will also vary with mean flow velocity.

3.2. Flow reattachment point

The most significant change in flow over dunes in these experiments concerns the point of flow reattachment. Herein, the reattachment point was calculated for each condition by finding the streamwise location of the highest time-average magnitude in flow vorticity at the bed. The length of the shear layer, and thus reattachment point, for Runs 2-5 shows some systematic variation (plotted as distance from the crest to the near-bed vorticity maximum, Figure 2). The slowest condition (Run 1, 0.14 ms^{-1}, Re=38535) does not fit this trend and given the very low velocities in this run may display different interacting processes (see discussion).

3.3 Quadrant Analysis

Quadrant analysis was performed using the same methodology applied in Bennett and Best (1995) with a threshold value (hole size) of one standard deviation. Figure 3 (see end of article) displays contour plots of the quadrants (% contributions) for two runs; Run 1 (0.14 ms^{-1}, Re=38535) and Run 3 (0.70 ms^{-1}, Re = 194491), displayed in the left and right series of panels of Figure 3 respectively, and shows the spatial change in the turbulent flow structure over the dune.
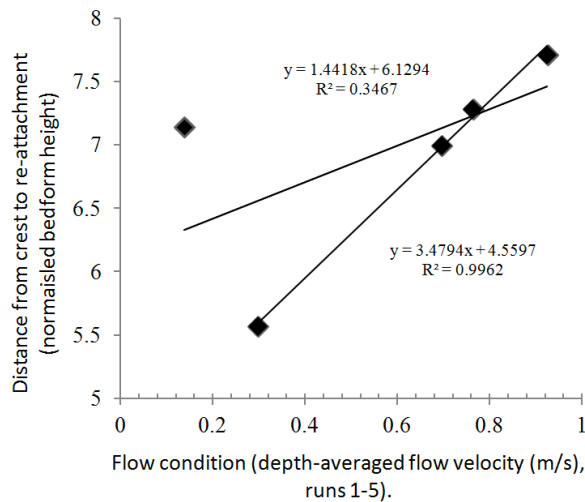
Figure 2: Reattachment length for Runs 1-5.

Quadrants 2 and 4 neatly highlight the position of the shear layer and wake, with Q2 events (ejections) being concentrated into the separation zone and Q4 (inrushes) dominating along the shear layer interface for both conditions (Figure 3). There are, however, some distinct changes between the two runs, with Q4 in Run 1 being significantly more dominant across a larger area than in Run 3 where Q4 events are mostly confined to the shear layer and a zone just above the stoss side. The wake from the upstream bedform can be seen in the Q2 contours for both flow velocities shown here (above the crest). However, there is a significant change in the dominance and position of the wake between these two conditions. In Run 3, the Q2 region extends well beyond the downstream crest and stacks above the developing shear layer and boundary layer of the downstream dune stoss side, whilst this stacking is almost non-existent for the slower velocity Run 1. The wake stacking above a shear layer seen here is similar to that shown by Fernandez et al. (2006), where superimposed bedforms created two stacked shear layers that interacted to enhance the turbulence produced around the flow separation zone. Therefore, this phenomenon should lead to larger and more energetic eddies being produced along the shear layer and at flow reattachment and thus a likely increased bed shear stress through this zone, particularly given that the position of Q2 ejections along the whole stoss region of the downstream dune are closer to the bed for the higher velocity Run 3 (Figure 3D).

4. DISCUSSION

The overlapping nature of the normalised downstream (*u*) velocities (Figure 1) masks a significant amount of variability in the flow field data presented herein. The differences in the normalised vertical (*w*) velocities provide an indication of the scale of relative change in the flow structure with increasing mean flow velocity and flow Reynolds Number. These results also demonstrate how strongly the bedform shape controls the velocity profiles in, and near, the shear layer. Nevertheless, the systematic increase in reattachment length with increasing flow velocity for Runs 2-5 shows that this phenomenon does change with flow velocity and is not just controlled by bedform geometry as described by Kadota and Nezu (1999). The variation between Runs 2-5 and run 1 is possibly explained by the lack of a wake overlapping the shear layer (as shown by quadrant analysis). Nelson et al. (1993, 1995) discuss the importance of the wake region on the stoss of dunes in controlling the initiation, growth and stability of dunes. This region is subject to a developing boundary layer due to the flow reattachment zone of the preceding separation zone, and the turbulent events that emanate from this zone. These pulses of turbulent flow produce localised high bed shear stress events that are responsible for the majority of sediment motion on the stoss of dunes (Nelson et al., 1993, 1995).

The spatial variation in quadrant contributions to the flow between Runs 1 and 3 (Figure 3 A,C,E,F for Run 1, B,D,F,H for Run 3) displays the dramatic changes that occur due to increasing flow velocity and Reynolds number. There is a major shift in the stacking of wake structures (notably Q2 events) with the increase in mean flow velocity. This stacking will result in enhanced turbulence as the wake zones from neighbouring dunes interact, which in turn will likely result in enhanced bed shear stresses in the flow recovery zone on the dune stoss side. A similar phenomenon is described by Fernandez et al. (2006) for superimposed bedforms. These results therefore begin to explore the relationships between flow structure zonation, bed shear stress and bedform morphology, and how these relations alter away from a flow-morphology equilibrium conditions.

267

5. CONCLUSIONS

Quantification of out-of-equilibrium flow over fixed, idealised, 2D dunes indicates that:

1. An increase in mean flow velocity causes substantial migrations in the locations of maximum turbulence generation and dissipation.

2. This change in turbulence zonation does not extend to, and does not appear to have a significant impact on, the height of flow separation. There is a possible relationship between increasing mean flow velocity and the length flow separation zone.

3. The flow field downstream of reattachment changes with flow velocity and Reynolds number. The zone of Q2 events extends downstream of the crest over the lee side separation region and also moves closer towards the bed over the subsequent dune stoss, which has significant implications for bed shear stress distributions and thus sediment dynamics.

4: The presence of wake stacking, from upstream dunes, over the flow separation region in the lee of the dune can occur without a change in bedform geometry and will likely contribute to morphological adjustment on the dune stoss side in response to flow variability.

6. ACKNOWLEDGMENTS

7. REFERENCES

Bennett, S. J. and Best, J. L. 1995. Mean flow and turbulence structure over fixed, two-dimentional dunes: implcations for sediment transport and bedform stability. *Sedimentology,* 42**,** 491-513.

Best, J. 2005a. The fluid dynamics of river dunes: A review and some future research directions. *Journal of Geophysical Research,* 110.

Best, J. 2005b. The kinematics, topology and significance of dune-related macroturbulence: Some observations from the laboratory and field. *In:* Blum, M. D., Marriott, S. B. and Leclair, S. (eds.) *Fluvial Sedimentology VII* Special Publication of the International Association of Sedimentologists.

Fedele, J. J. and Garcia, M., H. 2001. Alluvial roughness in steams with dunes: A boundary-layer approach. *In:* Seminara, G. and Blondeaux, P. (eds.) *River, Coastal and Estuarine Morphodynamics.* New York. Springer.

Fernandez, R., Best, J. and López, F. 2006. Mean flow, turbulence structure, and bed form superimposition across the ripple-dune transition. *Water Resources Research,* 42.

Garcia, M., H. (ed.) 2008. *Sedimentation Engineering,* Reston, Virginia, USA: American Society of Civil Engineers.

Garcia, D. (2011). A fast all-in-one method for automated post- processing of PIV data. *Experiments in Fluids.* 50,1247–1259.

Kadota, A. and Nezu, I. 1999. Three-dimensional structure of space-time correlation on coherent vortices generated behind dune crest. *Journal of Hydraulic Research,* 37**,** 59-80.

Mclean, S. R., Nelson, J. and Wolfe, S. R. 1994. Turbulence structure over two-dimensional bed forms: Implications for sediment transport. *Journal of Geophysical Research*, 99, 12,729-12,747.

Nelson, J.M, Shreve, R.L; Mclean, S.R, Drake, T.G. 1995. Role of Near-Bed Turbulence Structure in Bed Load Transport and Bed Form Mechanics. *Water Resources research,* 31, 8, 2071-2086.

Nelson, J., Mclean, S. R., Wolfe, S. R. 1993. Mean Flow and Turbulence Fields Over Two Dimensional Bed Forms. *Water Resources Research,* 29**,** 3935-3953.

Nezu, I., Nakagawa, H. 1993. *Turbulence in Open Channel Flows.,* Rotterdam, A.A. Balkema.
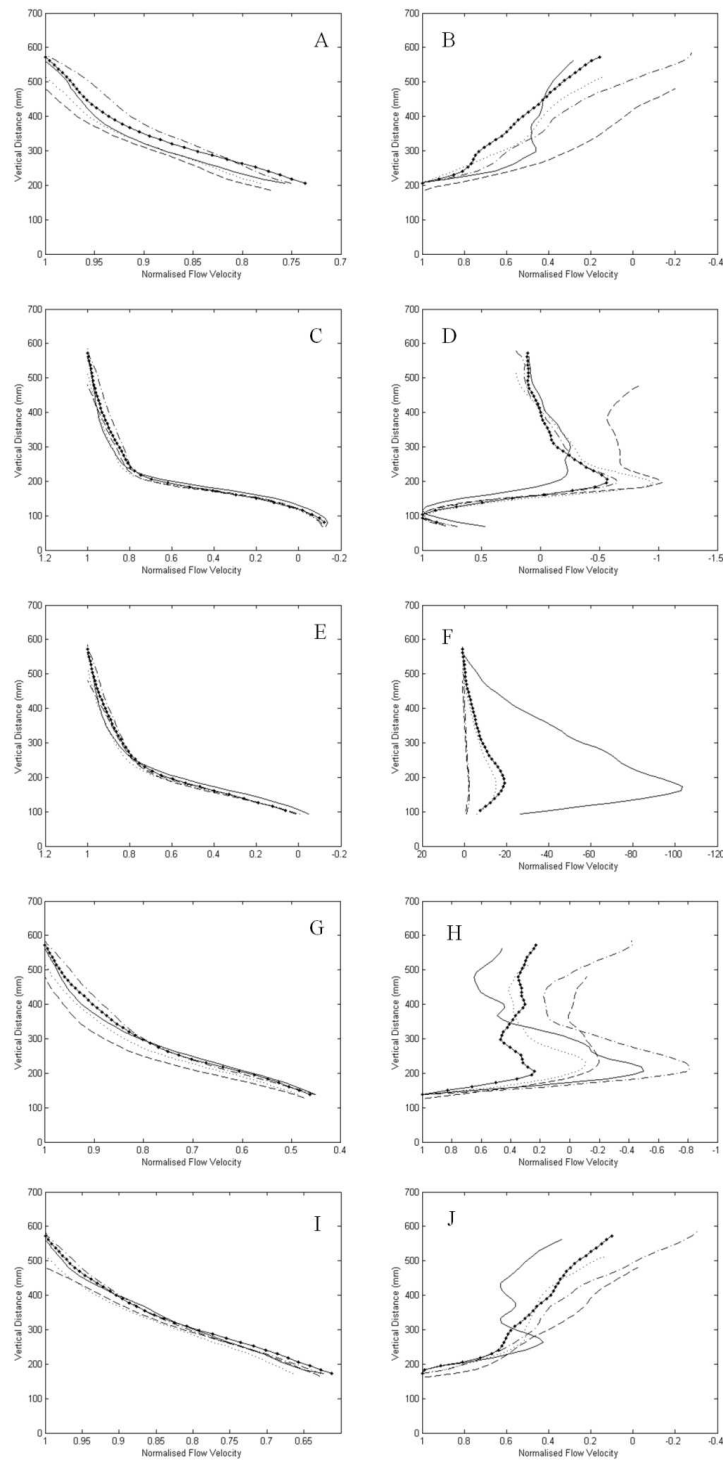
Figure 1: Normalised time-averaged velocity profiles with streamwise velocity component *u* (left) and vertical component *w* (right). Sequence A-E shows different locations across the dune (A-B y= 180 (at crest); C-D y= 400, (at trough); E-F y= 650 (near reattachment), G-H y=1200 (at mid-stoss of downstream dune), I-J y=1500 (upper stoss)). Solid black = 0.14ms^{-1}, line-diamonds = 0.30ms^{-1}, small-dash = 0.70 ms^{-1}, dot-dash = 0.76ms^{-1}, large-dash = 0.92ms^{-1}. Y axis is the vertical height in mm, X axis is normalised by the maximum flow velocity for each run.
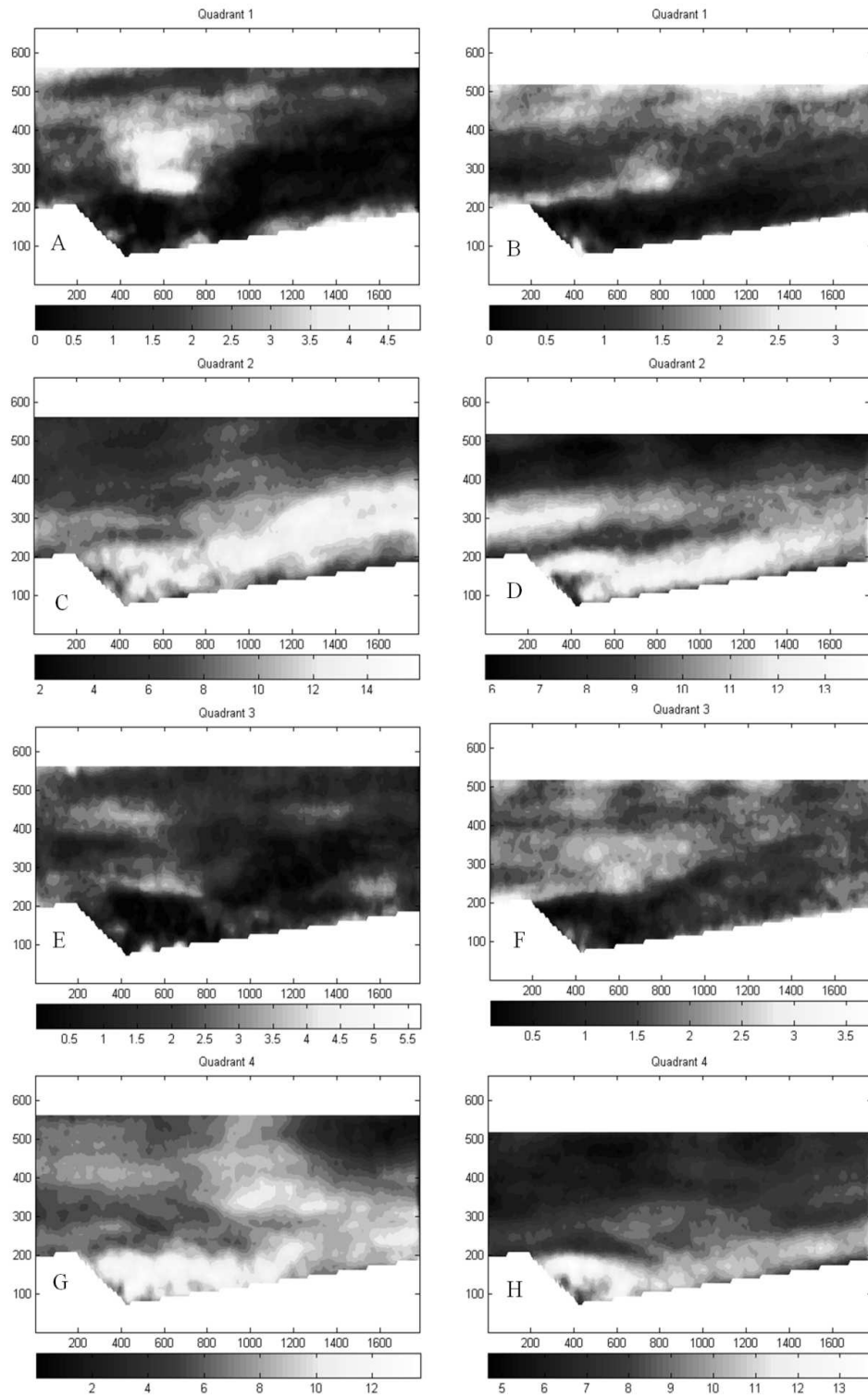
Figure 3: Quadrant analysis for Run 1 (left) and Run 3 (right) - A-B = Q1, C-D=Q2, E-F=Q3, G-H=Q4. Panels A,C,E and G are for Run 1 (at 0.14ms⁻¹) and Panels B,D,F,H are for Run 3 (at 0.7ms⁻¹). Note the changing contour values between panels. X and Y axis labels refer to distances in mm.